photonics

MDPI

Article

Sample Delivery Systems for Serial Femtosecond Crystallography at the PAL-XFEL

Jaehyun Park [1,2,*] and Ki Hyun Nam [3,4,*]

[1] Pohang Accelerator Laboratory, Pohang University of Science and Technology, Pohang 37673, Republic of Korea
[2] Department of Chemical Engineering, Pohang University of Science and Technology, Pohang 37673, Republic of Korea
[3] Department of Life Science, Pohang University of Science and Technology, Pohang 37673, Republic of Korea
[4] POSTECH Biotech Center, Pohang University of Science and Technology, Pohang 37673, Republic of Korea
* Correspondence: jaehyun.park@postech.ac.kr (J.P.); structures@postech.ac.kr (K.H.N.)

Abstract: Serial femtosecond crystallography (SFX) using an X-ray free electron laser (XFEL) enables the determination of room-temperature structures without causing radiation damage. Using an optical pump-probe or mix-and-injection, SFX enables the intermediate state visualization of a molecular reaction. In SFX experiments, serial and stable microcrystal delivery to the X-ray interaction point is vital for reasonable data collection and efficient beam time. The Pohang Accelerator Laboratory X-ray Free Electron Laser (PAL-XFEL) facility established SFX instruments at a nanocrystallography and coherent imaging (NCI) experimental station. Various sample delivery methods, including injection, fixed-target scanning, and hybrid methods, have been developed and applied to collect XFEL diffraction data. Herein, we report the currently available sample delivery methods for SFX at the NCI experimental station at the PAL-XFEL. This article will help PAL-XFEL users access the SFX system for their experiments.

Keywords: serial femtosecond crystallography; X-ray free electron laser; sample delivery; injector; fixed-target scanning; hybrid method

Citation: Park, J.; Nam, K.H. Sample Delivery Systems for Serial Femtosecond Crystallography at the PAL-XFEL. *Photonics* **2023**, *10*, 557. https://doi.org/10.3390/photonics10050557

Received: 15 April 2023
Revised: 8 May 2023
Accepted: 9 May 2023
Published: 10 May 2023

1. Introduction

Structural biology provides intuitive information for understanding life phenomena based on biomolecule structure [1–4]. Biophysical techniques such as macromolecular X-ray crystallography (MX), nuclear magnetic resonance (NMR), cryogenic electron microscopy (cryo-EM), and microcrystal electron diffraction (MicroED) have been used to determine the structure of biomolecules [5,6]. Among these, MX has the advantage of being able to observe molecules at the atomic resolution level and has made the greatest contribution to the field of structural biology [7,8]. Cryo-EM has recently gained considerable attention in the field of structural biology [9]. Technological advances have enabled a level of resolution that can identify molecular functions and is expected to contribute substantially to the field of biology in the future [10]. Although these MX and cryo-EM techniques have contributed significantly to the field of structural biology, problems regarding biologically unreliable structural information may arise owing to experimental radiation damage and cryogenic environments during experiments [11,12].

These technical limitations can be overcome using serial femtosecond crystallography (SFX) with an X-ray free-electron laser (XFEL) source [13]. An XFEL provides ultrashort X-ray pulses and has the advantage of avoiding radiation damage based on the "diffraction before destruction" principle [14]. In addition, high-resolution diffraction is possible using small crystals owing to the intense X-ray peak power [15]. Moreover, because a typical SFX experiment delivers and exposes a crystal sample to an X-ray position at ambient

temperature, the collected diffraction data contain room-temperature structural information, which in turn provides useful information on the molecular flexibility or fluctuation [16,17].

Furthermore, the reaction process of the target molecule can be observed at various time delays using either an optical pump-probe experiment or a mix-and-inject technique that mixes a substrate or inhibitor with crystal slurries [18–21]. The time-resolved SFX accompanied by the previous techniques is advantageous for determining the molecular mechanisms of biological reactions [22,23]. Accordingly, the SFX technique provides experimentally reliable structural information when compared with other structural biology techniques [24].

In the MX experiment, sample delivery involved simply mounting a single crystal on a goniometer, and three-dimensional (3D) diffraction data were collected by rotating the crystal [25]. In SFX, numerous microcrystals with random orientations must be delivered to the X-ray interaction point in a serial and stable manner under perfect humidity conditions to collect the diffraction data [15,26]. Therefore, the development of a simple and efficient sample delivery system is required. Various sample delivery methods, such as liquid jet injectors, injectors or syringes with viscous media, and fixed-target scanning have been developed and applied to SFX data collection [27–29]. An appropriate sample delivery method can be selected according to the research purpose, sample characteristics, sample environment, and XFEL characteristics (e.g., repetition rate).

To date, there are five hard X-ray XFEL facilities worldwide, one of which is the PAL-XFEL, located in Pohang, South Korea [30,31]. The PAL-XFEL is currently operating at two experimental stations for hard X-ray regimes [30,32]. The SFX instruments were installed in the NCI experimental station at the hard X-ray beamline of the PAL-XFEL [33,34]. Table 1 summarizes the specification of the experimental parameters of the SFX instrument at PAL-XFEL.

Table 1. Specification of SFX experimental endstation at the PAL-XFEL.

Parameter	Specification
X-ray energy (keV)	6–15
Energy bandwidth (%) at 9.7 keV	SASE: ~0.2 Self-seeding: ~0.002
Pulse duration (fs)	<25
Photon flux (photons/pulse)	$>10^{11}$ at 9.7 keV (SASE mode)
Repetition rate	Up to 60 Hz
Beam size (μm, FWHM) at the sample position	~2 (H) X 2 (V) at 12.4 keV
Sample chamber	MICOSS, fixed target (FT) chamber
Sample delivery	Fixed target (1D, 2D), PSD injector, CMD injector, MLV injector
Sample environment	Ambient pressure at room temperature (helium gas purging)
Sample position manipulation	XYZ motion with a combination of 3 linear stages
X-ray detector	Rayonix MX225-HS, Jungfrau 4M
Data analysis software	Cheetah, CrystFEL, Phenix, CCP4i, ADXV, OnDA

The SFX science program at the PAL-XFEL now operates a conventional SFX to determine room-temperature structure without radiation damage as well as a time-resolved SFX to identify molecular reactions in the time domain. We have demonstrated several sample delivery methods, such as injection, fixed-target scanning, and hybrid methods, by determining the room-temperature structure of macromolecules [35–41].

Here, we introduce sample delivery methods developed for the SFX science program at PAL-XFEL. We discuss their applications to data collection and describe some sample delivery instruments: new ones currently under development and others that can

be improved. This article will be useful for those who wish to understand the current state of SFX applications, as well as for those who plan to utilize a specific sample SFX delivery instrument.

2. SFX Sample Delivery Systems

2.1. Injector

In the early stages of injector sample delivery for SFX, liquid flow has mainly been controlled with pressurized liquid pumps. For a crystal suspension in solution, a liquid jet injector is used in combination with a gas dynamic virtual nozzle (GDVN) to create a narrow continuous jet with a diameter of a few microns [35,42]. This has an advantage in terms of sample stability because it maintains the crystallization conditions, but it requires a fast flow rate to create a stable stream. Therefore, sample consumption is high when applied to PAL-XFEL with a maximum repetition rate of 60 Hz or synchrotron. In the case of samples that are crystallized in lipidic cubic phase (LCP) and viscous media mixed with tiny crystals, the flow rate can be much lower than that with a liquid jet [26]. However, chemical or physical reactions between the crystal sample and viscous substance may cause damage to the crystal sample and lower the viscosity of the viscous substance [26]. Accordingly, injector techniques require a way to test a suitable injector or viscous material before data collection.

2.1.1. Injector System

All injector systems developed at the PAL-XFEL can be installed and operated in a multifarious injection chamber for molecular structure study (MICOSS) (Figure 1a) [35]. The MICOSS system consists of three-axes translation stages to align the injection stream to the X-ray beam path, as well as two in-line camera systems to monitor the two-dimensional positions of the liquid stream, parallel and perpendicular to the incident XFEL pulses. The inner space of the MICOSS is isolated from the outside of the chamber to maintain a low vacuum or helium purging environment; therefore, the injection stream is not affected by the external air flow in the experimental hutch [35]. To date, three different injection methods have been applied to SFX instruments at PAL-XFEL: (i) particle solution delivery (PSD) injectors [35], (ii) carrier matrix delivery (CMD) injectors [35], and (iii) microliter volume (MLV) syringe injectors [32].

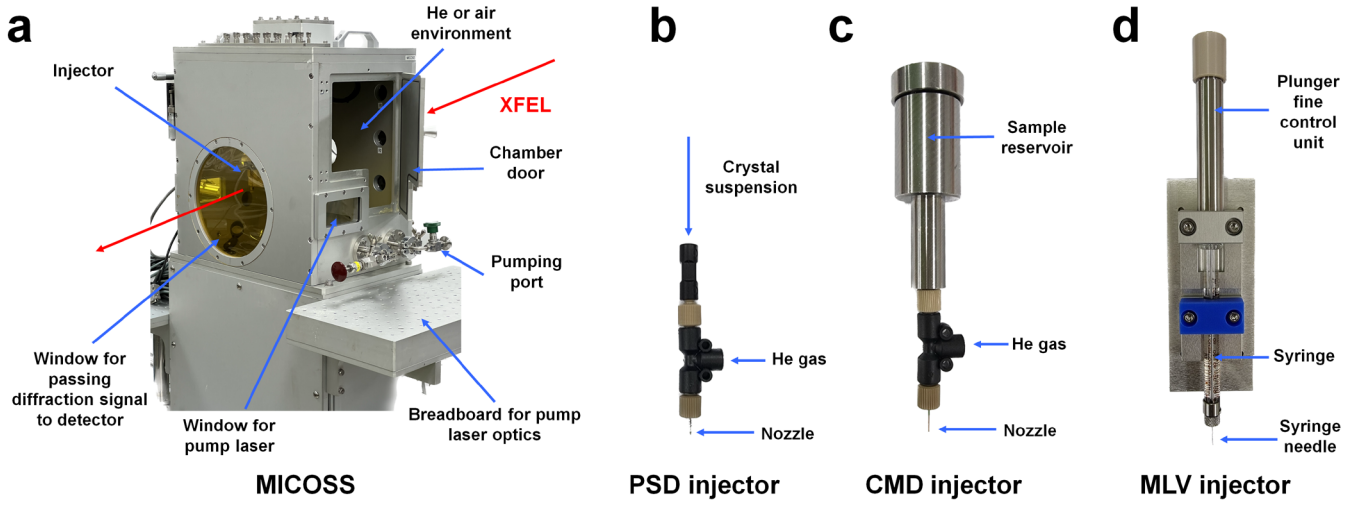

Figure 1. Injector system for serial femtosecond crystallography (SFX) at the PAL-XFEL. Photograph of: (**a**) multifarious injection chamber for molecular structure study (MICOSS) chamber, (**b**) particle solution delivery (PSD) injector, (**c**) carrier matrix delivery (CMD) injectors, and (**d**) microliter volume (MLV) syringe injector.

A PSD injector was developed to deliver a solution or crystal suspension sample [35]. In the PSD injector nozzle, the target sample was delivered via a tapered capillary surrounded by a gas-focusing capillary with coaxial geometry. Various inner diameters of the tapered capillary (50, 75, 100, 150, and 200 μm) were prepared, which could be selected depending on the type or size of the target molecules [35]. PSD injection was successfully applied to the SFX experiment during the commissioning period of the PAL-XFEL. However, high flow rates of about 20–30 μL/min are required to create a stable liquid stream. Considering the PAL-XFEL repetition rate, more sample portions should be unexposed to XFEL pulses. Therefore, PSD injectors are currently not favored owing to unwanted high sample consumption, but they can be used in experiments with current chemical solutions. To create a stable injection stream at a low flow rate, a crystal delivery method using viscous materials is widely used in XFEL facilities and synchrotrons with low repetition rates. A CMD injector was developed to stably deliver crystals embedded in viscous materials at low flow rates [35]. The body of the CMD injector was made of stainless steel and the volume of the sample reservoir is 40 μL [35], which was delivered for approximately 6.6 h at a flow rate of 100 nL/min. The CMD injector has a helium gas flow with a coaxial geometry to maintain the nozzle structure and injection stream from which the sample is ejected, similar to the PSD injector [35]. The inner diameters of the available nozzles were 75, 100, and 150 μm to deliver different crystal sizes [35].

In addition, we developed a microliter volume (MLV) syringe injector to deliver a viscous medium containing microcrystals [32]. During sample preparation for injection with the viscous medium, microcrystals and viscous medium were mixed in a dual-syringe setup with a syringe coupler. The prepared syringe, containing microcrystals embedded in the viscous medium, can be directly used as an injector without transferring the sample to a CMD injector reservoir. Accordingly, the sample preparation step from the user side was simplified, and the experiment efficiency was increased. The MLV syringe injector is operated by transmitting pressure from a high-performance liquid chromatography (HPLC) pump to the syringe plunger of the MLV syringe injector [32]. This MLV syringe system is currently the preferred injector system according to recent PAL-XFEL users.

2.1.2. Viscous Medium

Various types of viscous materials, such as LCP and hydrophobic and hydrophilic delivery media, have been developed for serial crystallography [26]. These materials can be selected and used based on the research purpose and the characteristics of the crystal samples. It is important to select a viscous material that does not interact with the crystal sample to avoid damage to the sample or a change in viscosity owing to a chemical reaction between the sample and the medium [26]. Polyacrylamide (PAM) is widely used for electrophoresis in biological experiments because it does not interact with proteins or nucleic acids [43]. Thus, a polyacrylamide (PAM) injection matrix was developed based on these characteristics. We have successfully determined the native structures of lysozyme and thermolysin utilizing the PAM injection matrix as a carrier medium, using the CMD injector at PAL-XFEL (Figure 2a) [37]. However, the viscosity of PAM fragments is not high enough to create a stable injection stream; instead, it requires a relatively high flow rate of 0.8–1 μL/min [37]. To overcome this issue, we have developed other viscous media such as shortening [44], wheat starch [45], alginate [45], lard [46], and beef tallow [47], which have a higher viscosity than polyacrylamide. These viscous media have been developed using the serial synchrotron crystallography (SSX) technique at PLS-II because of the limited beamtime at the XFEL facilities. These viscous materials are expected to be applicable to SFX experiments; however, it is necessary to confirm whether they can be applied to PAL-XFEL because there is a difference in beam characteristics and intensity between synchrotron X-rays and XFEL. Among them, the lard injection matrix was applied in PAL-XFEL for the delivery of xylanase crystals (Figure 2b) [48]. The results showed that there was no significant problem for data collection and processing in terms of the stability of the injection stream and X-ray background scattering [48]. Thus, we conclude that viscous

materials previously developed in PAL-XFEL and PLS-II can be applied in SFX experiments as sample delivery media.

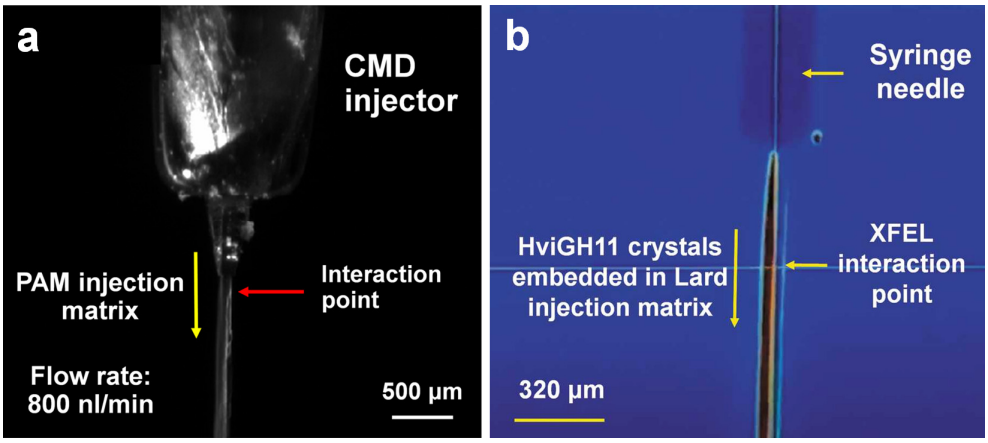

Figure 2. Injection of viscous medium containing the crystals at serial femtosecond crystallography (SFX) instrument at Pohang Accelerator Laboratory X-ray Free Electron Laser (PAL-XFEL). (**a**) Injection of polyacrylamide (PAM) injection matrix by carrier matrix delivery (CMD) injector. The original figures were obtained from a previous study [37]. (**b**) Injection of lard injection matrix by microliter volume (MLV) injector. Reproduced with permission of the International Union of Crystallography [48].

The reservoir volume of the sample in PSD, CMD, and MLV injectors are 10 mL, 40 μL, and 100 μL, respectively. When the X-ray hit rate of the crystal or the diffraction intensity is high, the sample reservoir volume in each of these injectors is sufficient to collect images that can determine the three-dimensional structure. However, when the hit rate of the diffraction image is low or does not reach the structural resolution desired by the researcher, more data will need to be collected. Accordingly, when using the injection system for SFX, the required crystal sample volume will be determined depending on the crystal density and diffraction intensity.

2.2. Fixed-Target Scanning

Fixed-sample scanning is a method in which crystals are sprayed onto the sample holder, and the crystal sample is delivered to the X-ray interaction point using motion stages. This technique allows lower sample consumption than the previous injector system and minimizes physical damage to the crystals during the sample preparation and delivery processes [27,49]. Another advantage is that samples can be delivered to the XFEL interaction point at the desired speed and timing using motion control software [27,49]. To date, various types of fixed-target scanning methods have been developed and applied to SFX data collection at PAL-XFEL [36,38,39].

2.2.1. Nylon-Mesh Sample Holder

Nylon is composed of a polyethylene segment that transmits X-rays [50]. As this material exhibits low background scattering when X-rays pass through it, it is widely used to mount single crystals in macromolecular crystallography in the form of nylon loops [51,52]. However, if many crystal samples are mounted on the nylon loop used in MX, the crystal samples may sink downward owing to gravity. To solve this problem, a nylon mesh was used to prevent sinking by settling on each mesh pore of the crystal samples when the crystals were sprayed from the sample holder [36] (Figure 3a). Nylon mesh is commercially available and produced in a variety of pore sizes; therefore, users can select it according to their crystal size. To avoid dehydration damage to the samples, the nylon mesh containing crystals was enclosed by polyimide films [36]. This sample chip can be handled without dehydration, even if left in contact with air for several days (Figure 3b). The sample chip was mounted on translation stages inside the FT-SFX chamber; it was moved in a raster

motion in the vertical and horizontal directions and enabled the collection of diffraction data. The prepared chip generated two kinds of background scattering patterns: one from the nylon material (positions around 3.75 and 4.30 Å), and circular scattering from the polyimide film (near 15.3 Å) (Figure 3c). The room-temperature structures of lysozyme and glucose isomerase were successfully determined using a nylon mesh sample holder. In previous studies, thicknesses of approximately 20 µm for nylon mesh and 25 µm for polyimide films were used. Their background scattering did not interrupt the indexing of diffraction patterns or the determination of the structures. However, if it is a challenge to get weaker signals, thinner nylon and polyimide films should be considered. Additionally, to minimize scattering from the solvent, a thinner frame holding the chip can be used to reduce the sample volume. In this study, a nylon mesh was used to settle the crystals, but it can be replaced with a material that transmits X-rays and has low background scattering, such as polyimide mesh [53,54]. Similarly, to prevent dehydration, polyimide films can be replaced with materials such as Mylar [55] and synthetic cyclic olefin copolymer (COC) [56]. Currently, nylon-mesh sample holders are widely used for diffraction data collection in serial femtosecond crystallography.

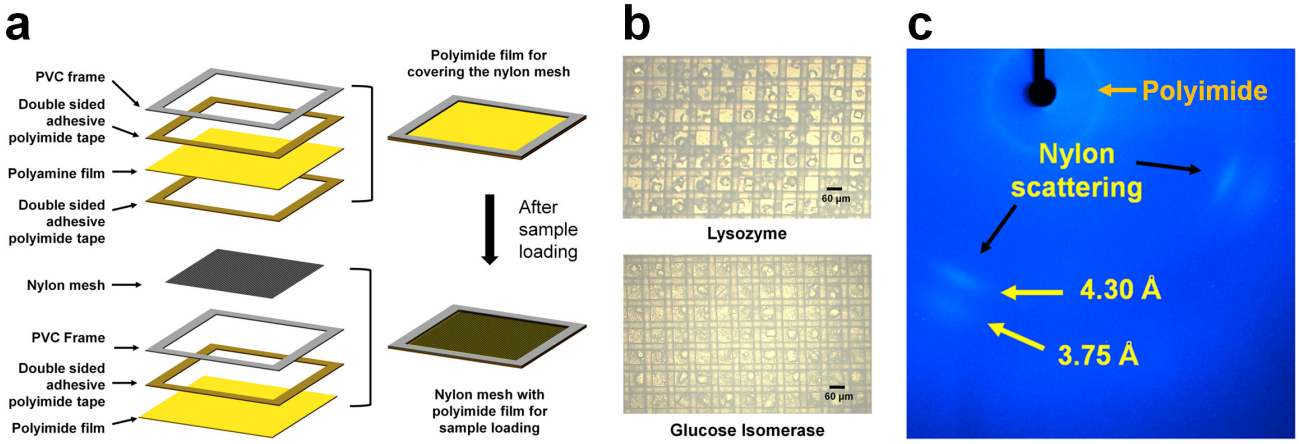

Figure 3. Nylon mesh-based sample holder. (**a**) Schematic of the composition of the nylon mesh-based sample holder. (**b**) Photograph of crystal suspension in nylon-mesh sample holder. (**c**) Background scattering of nylon-mesh sample holder. The original figures were obtained from a previous study [36] and have been modified.

2.2.2. Microcrystal Container (MCC)

The MCC is composed of polyimide micro-tubing which is stable against various chemicals (Figure 4a). The crystal suspension was injected into the micro-tubing using a syringe [38]. The tubing had a thickness of 13 µm, and the background scattering generated during XFEL transmission did not affect data processing [38]. The inner diameter of the tubing was 100 µm, and because of the cylindrical structure of the tubing, the background scattering of the solvent was high when the XFEL passed through the center. Crystal samples placed in the tubing sink owing to gravity, and exposure of the XFEL to the bottom of the tubing results in a relatively high crystal hit rate and low solvent background scattering. Crystal samples can be seated in various orientations using a curved bottom at the bottom of the cylindrical tubing (Figure 4b) [38]. Because both ends of the MCC containing the crystal suspension were sealed with glue, the samples remained perfectly hydrated and problems such as crystal clogging in the injector were absent. The MCC containing the crystal was installed on an MCC mounting chip composed of an acrylic plate. The length of the tubing installed in the horizontal direction on the MCC chip was 56 mm and multiple MCCs were installed in the vertical direction. During data collection, the MCC was scanned in the horizontal direction to collect diffraction data; then, it moved in the vertical direction, and the next MCC was scanned to collect data. The MCC chip may not be perfectly aligned in the horizontal direction during mounting in the sample chamber stage.

Even when these MCC chips are slightly tilted during the mounting process, the XFEL may not illuminate the micro-tubing. To overcome this tiny mis-alignment issue during the raster scanning, a fast position feedback process—a real-time visual servo method—is applied to the MCC chip (Figure 4c) [38]. It recognizes the MCC image and aligns the MCC chip in real time, allowing the XFEL to penetrate the MCC perfectly.

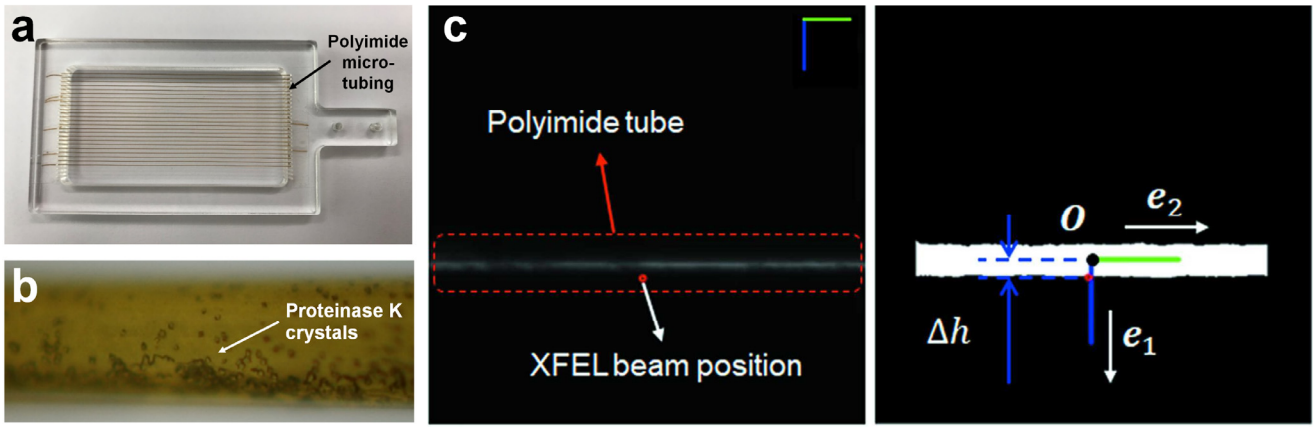

Figure 4. Microcrystal container (MCC) sample delivery system. (**a**) MCC chip. (**b**) Microscopic view of MCC containing the proteinase K crystals. (**c**) Snapshot image of MCC using the vision acquisition module. Reproduced with permission of the International Union of Crystallography [38].

2.2.3. Viscous Medium Supporter

In a fixed-target (FT) sample holder, crystals can be seated in a preferred orientation depending on their shape, which requires more data collection to obtain 3D structural information or even makes structural determination impossible [39]. In addition, when the size of the crystals is random or very large, it is inefficient to set them in conventional sample holders with regular-sized holes [39]. Therefore, it is important to allow samples of different sizes and crystals to settle in random orientations. To overcome this issue, we developed a crystal support based on a viscous material (Figure 5) [39]. The crystal samples were embedded in a viscous medium, such as agarose or gelatin, and enclosed in a polyimide film to avoid dehydration [39]. Viscous materials containing crystals can be stably placed between polyimide films without sinking owing to gravity. Consequently, this method replaced the viscous material with a nylon mesh, on which the crystals were deposited in the previous nylon-mesh sample holder [36]. To apply this experimental technique, the crystal sample must be physically safe while mixing with viscous substances and must not lower the viscosity of the viscous medium. Agarose and gelatin were used in this demonstration experiment; however, they could be replaced with other delivery materials, depending on the type or characteristics of the crystal. In addition, because background scattering occurs when X-rays pass through viscous materials, a thinner viscous material in the sample holder is important to produce low background scattering from the viscous medium.

2.3. Hybrid Method

All sample delivery systems have unique advantages and are selected and used according to the experimental environment, sample type, and research purpose. In general, a sample delivery device using an injector has the advantage of the continuous delivery of fresh samples [35,42]. The fixed-sample scanning method has the advantage of being able to program and transfer the crystal sample to the desired location as an X-ray interaction point [49]. Using the advantages of injection and fixed-target scanning systems, a combination of inject-and-transfer systems (BITS) was developed at the PAL-XFEL [40,41].

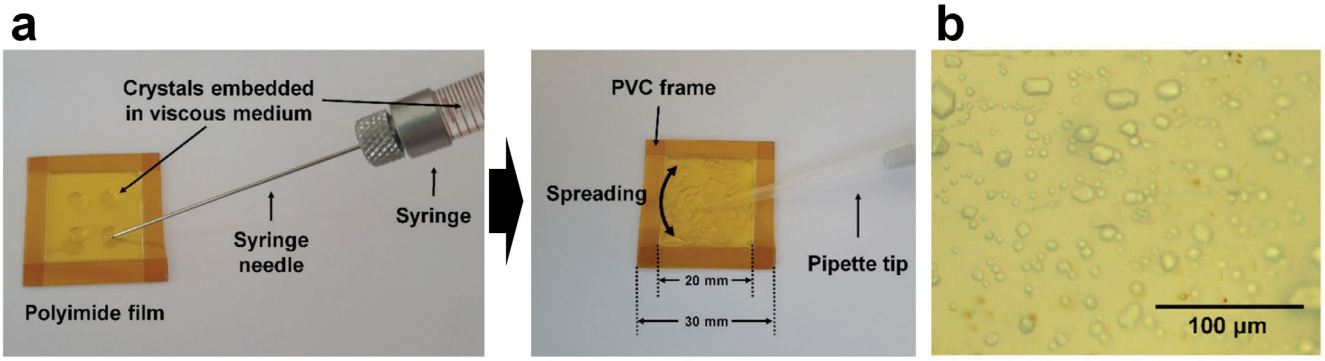

Figure 5. Viscous medium-based crystal support for fixed-target serial femtosecond crystallography (FT-SFX). (**a**) Photograph of the injection of crystals embedded in a viscous medium on polyimide film. (**b**) Crystals on a viscous medium based crystal support sample holder. Reproduced with permission of the International Union of Crystallography [39].

2.3.1. BITS

The BITS system collects data by depositing a crystal sample injected from an injector onto a polyimide film and then moving the crystal sample deposited on the film to the X-ray position using a translation stage (Figure 6a) [40]. The film on which the crystals were deposited was made of polyimide to reduce background scattering. It has a hydrophobic surface; therefore, crystal samples with hydrophilic properties were not stably deposited. To solve this problem, the polyimide film was subjected to ultraviolet ozone (UVO) treatment to increase the hydrophilicity of its surface, enabling stable crystal sample deposition (Figure 6b) [40].

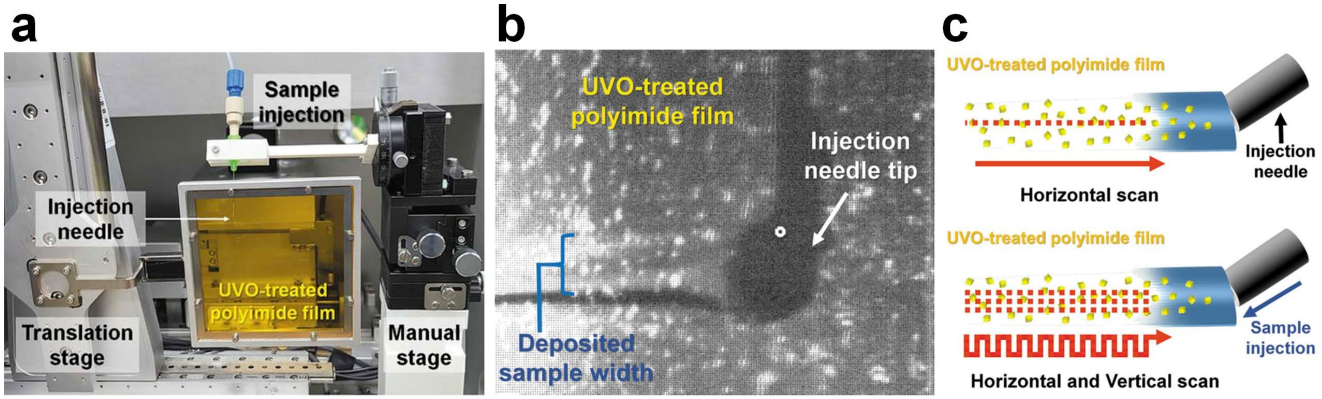

Figure 6. Combination of inject-and-transfer system at the Pohang Accelerator Laboratory X-ray Free Electron Laser (PAL-XFEL). (**a**) Experimental BITS setup. (**b**) Snapshot of the deposition of the injected sample on the UVO-treated polyimide film. (**c**) Vertical and horizontal scanning method in BITS. Reproduced with permission of the International Union of Crystallography [40].

Common injection techniques require the creation of an injection stream to deliver the sample stably and continuously to the X-ray location. However, in BITS, because the sample injected from the injector settles on the film, there is no need to create an injection stream, and it is possible to deliver the sample even at a low flow rate. An injection test on a BITS system showed that the sample could be stably deposited even at a flow rate of 1 pL/min [40]. However, it is important to maintain constant humidity because of crystal sample dehydration when delivered at a low flow rate in an ambient environment. The crystal sample deposited on the film in the BITS was wider than the inner diameter of the injection nozzle [40]. When the translator scans only in the horizontal direction, according to the sample to be injected, many sample parts are not exposed to X-rays. However, in BITS, it is possible to scan all deposited samples as it can be programmed to scan the deposited

samples both horizontally and vertically (Figure 6c). This unique data collection strategy, which can only be performed at the BITS, results in lower sample consumption than other injection or fixed-target scan techniques. In a previous study, when a crystal suspension was applied during data collection in a BITS system, the sample tubing was clogged by crystals. This problem was solved by mixing a viscous medium to prevent the tubing from clogging owing to the gravity of the crystal sinking and accumulation. The crystals were mixed with the lard injection matrix, delivered using the BITS system, and diffraction data were collected. In this experiment, the room-temperature lysozyme structure was determined with a sample volume of 1.4 μL in the BITS system [40]. Although we solved the clogging issue in BITS by mixing with a viscous medium, this system can be applied to crystal suspensions for other extended science programs, such as chemical mixing. To avoid crystal clogging in BITS, the length of the tubing between the syringe and syringe needle was minimized to reduce the space of the crystal sinking in the tubing. Moreover, it is necessary to increase the sample delivery efficiency by connecting a device, such as an anti-settler, to prevent the crystal from sinking into the syringe where the crystal is stored. Currently, the SFX endstation at PAL-XFEL has developed an anti-settler device that can rotate the sample holder containing the crystal sample in the perpendicular direction, which can be applied in future experiments that require crystal sinking prevention.

2.3.2. Upgraded BITS

In the first version of BITS, the position of the injection needle tip was aligned using the manual stage. In an extended study, all translation motions were updated to a motorized stage, a graphical user interface (GUI) for translator operation was developed, and the related coding sources were reported [41]. In addition, by mixing and injecting a material with high viscosity, such as PEG300 or PEG4000, into the crystal sample, an attempt was made to eliminate the pretreatment process by depositing it on a hydrophobic polyimide film without UVO treatment [41]. The injection experiment showed that the solution sample was stably mounted when it was composed of more than 10% (w/v) PEG 3350 or PEG 6000 [41]. When the crystal suspension contains a high concentration of viscous precipitant or if the crystal is physically stable when added to the highly viscous precipitant, the preparation process for the experiment in BITS can be simplified because the UVO treatment of the polyimide film is omitted. Previously, a single syringe was used to deliver the crystal samples [40], whereas in the upgraded BITS, the syringe needle holder was 3D printed and designed to install two syringe needles (Figure 7) [41]. The tips of the two syringe needles were in contact with each other; lysozyme crystals were injected from one syringe, and sugar molecules, inhibitors of lysozyme, were mixed with the other syringe [41]. Although sufficient diffraction data to determine the complete three-dimensional structure were not collected owing to clogging in the tubing, mixing of the two materials from the two syringes was observed [41]. This is an inject-and-diffuse method, because the sample is injected from two syringes and then diffused on the UVO-treated polyimide film. Because this method uses the diffusion of two samples rather than physical mixing, it will be useful for time-resolving experiments with slower reaction rates than the existing mix-and-injection technique for fast reactions. To shorten the reaction time, an injector can be used after mixing the two samples, such as a mixing injector [57–59]. In contrast, the injection-and-mix method may vary depending on the sample environment, sample concentration, type, or characteristics of the solution (e.g., viscosity), and the affinity between mixed materials. Therefore, it is essential to pre-test the mixing efficiency of the crystals and chemical solution.

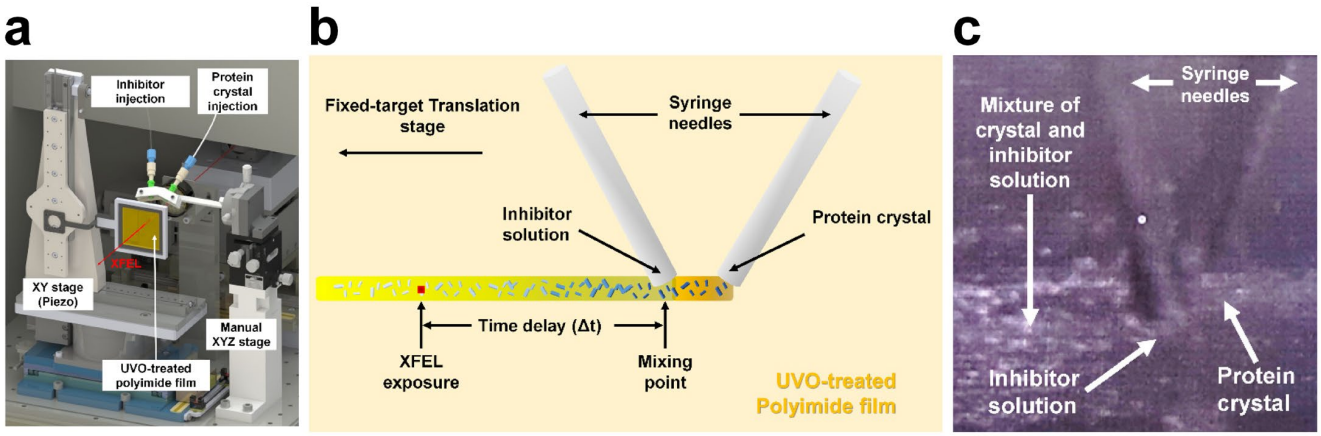

Figure 7. Upgraded inject-and-transfer system (BITS). (**a**,**b**) Experimental setup of the BITS with two-syringe installation. (**c**) Pilot experiment of inject-and-diffuse experiment in BITS. The original figures were obtained from a previous study [41].

3. Discussion

Because the SFX technique uses the characteristics of the XFEL's high peak power intensity and ultra-short pulse duration, it can provide the most biologically reliable structural information among the various structural biology techniques [24]. Time-resolved SFX experiments accurately reveal the reaction mechanisms of various biomolecules [22]. Herein, we describe the sample delivery methods developed and applied to PAL-XFEL. All these methods were applied to SFX refinement at the PAL-XFEL and successfully determined the room-temperature structure of several macromolecules at high-resolution, apart from PSD injection. Accordingly, the PAL-XFEL SFX user enabled the use of the demonstrated sample delivery system at the PAL-XFEL. The PSD injector also stably delivered the crystal suspension to the X-ray position, which was used during the commission at the PAL-XFEL. As mentioned above, the liquid jet injector has no advantage in terms of sample consumption for application to the PAL-XFEL with a low repetition rate because the sample is more overwhelming; therefore, the PSD injector can be applied in other studies using a solution or other megahertz XFEL facilities. We successfully demonstrated the performance of various developed sample delivery systems. All sample deliveries are continuously upgraded through feedback from the user site or operational experience. Our developed sample delivery methods, such as injection, fixed-target scanning, and hybrid methods, converged to a maximum repetition rate of 60 Hz from the PAL-XFEL. In terms of repetition rate, the sample delivery system developed at the PAL-XFEL can be applied in SACLA and SwissFEL facilities or synchrotrons. However, the developed sample delivery instruments are not optimal for European-XFEL or LCLS facilities when a megahertz repetition rate is offered. In addition, these sample delivery systems have also been applied to several time-resolved SFX with photoactive proteins and viscous injectors or fixed-target methods using optical laser pumps (not published). Moreover, the mix-and-inject and inject-and-diffuse methods are under development.

The PAL-XFEL SFX beamtime consists of a regular beamtime for user operation, and a PCS beamtime to screen crystal diffraction. In the case of PCS beamtime, because multiple users share the beamtime in a 0.5–1 shift (~6–12 h), the quality of the crystal is screened using fixed-target delivery with pre-installed instruments. In contrast, regular beamtime allows the researcher to select the sample delivery method developed by PAL-XFEL according to their research purposes. The PAL-XFEL SFX has a sufficient space in the sample environment to apply both the delivery device developed by the user and the self-developed sample delivery method. Accordingly, researchers should discuss proper sample delivery methods and sample environments with beamline scientists prior to the beamtime.

Author Contributions: Conceptualization, J.P. and K.H.N.; data curation, J.P. and K.H.N.; writing—original draft preparation, J.P. and K.H.N.; writing—review and editing, J.P. and K.H.N.; funding acquisition, J.P. and K.H.N. All authors have read and agreed to the published version of the manuscript.

Funding: This work was funded by the National Research Foundation of Korea (NRF) (NRF-2017M3A9F6029736 and NRF-2021R1I1A1A01050838 to K.H.N.) and Korea Initiative for Fostering University of Research and Innovation (KIURI) Program of the NRF (NRF-2020M3H1A1075314 to K.H.N.). This study was supported by ProGen (to K.H.N.).

Institutional Review Board Statement: Not applicable.

Informed Consent Statement: Not applicable.

Data Availability Statement: Data sharing not applicable.

Acknowledgments: We would like to express our gratitude to Yunje Cho, Jong-Lam Lee, Wan Kyun Chung, Donghyun Lee, Keondo Lee, Sangwon Baek, and Jihan Kim from POSTECH for their valuable contributions in developing the sample delivery techniques. We would like to thank Sehan Park, and Sang Jae Lee at the PAL-XFEL for their assistance during the demonstration of the sample delivery method.

Conflicts of Interest: The authors declare no conflict of interest.

References

1. Hu, C.; Almendros, C.; Nam, K.H.; Costa, A.R.; Vink, J.N.A.; Haagsma, A.C.; Bagde, S.R.; Brouns, S.J.J.; Ke, A. Mechanism for Cas4-assisted directional spacer acquisition in CRISPR–Cas. *Nature* **2021**, *598*, 515–520. [CrossRef] [PubMed]
2. Nam, K.H. Crystal structure of human brain-type fatty acid-binding protein FABP7 complexed with palmitic acid. *Acta Crystallogr. D Struct. Biol.* **2021**, *77*, 954–965. [CrossRef] [PubMed]
3. Hu, C.; Ni, D.; Nam, K.H.; Majumdar, S.; McLean, J.; Stahlberg, H.; Terns, M.P.; Ke, A. Allosteric control of type I-A CRISPR-Cas3 complexes and establishment as effective nucleic acid detection and human genome editing tools. *Mol. Cell* **2022**, *82*, 2754–2768.e5. [CrossRef] [PubMed]
4. Hu, C.; van Beljouw, S.P.B.; Nam, K.H.; Schuler, G.; Ding, F.; Cui, Y.; Rodríguez-Molina, A.; Haagsma, A.C.; Valk, M.; Pabst, M.; et al. Craspase is a CRISPR RNA-guided, RNA-activated protease. *Science* **2022**, *377*, 1278–1285. [CrossRef]
5. Dobson, C.M. Biophysical Techniques in Structural Biology. *Annu. Rev. Biochem.* **2019**, *88*, 25–33. [CrossRef]
6. Tsegaye, S.; Dedefo, G.; Mehdi, M. Biophysical applications in structural and molecular biology. *Biol. Chem.* **2021**, *402*, 1155–1177. [CrossRef]
7. Pomés, A.; Chruszcz, M.; Gustchina, A.; Minor, W.; Mueller, G.A.; Pedersen, L.C.; Wlodawer, A.; Chapman, M.D. 100 Years later: Celebrating the contributions of x-ray crystallography to allergy and clinical immunology. *J. Allergy Clin. Immun.* **2015**, *136*, 29–37. [CrossRef]
8. Blakeley, M.P.; Hasnain, S.S.; Antonyuk, S.V. Sub-atomic resolution X-ray crystallography and neutron crystallography: Promise, challenges and potential. *IUCrJ* **2015**, *2*, 464–474. [CrossRef]
9. Chiu, W.; Schmid, M.F.; Pintilie, G.D.; Lawson, C.L. Evolution of standardization and dissemination of cryo-EM structures and data jointly by the community, PDB, and EMDB. *J. Biol. Chem.* **2021**, *296*, 100560. [CrossRef]
10. Liu, S.A.; Hattne, J.; Reyes, F.E.; Sanchez-Martinez, S.; de la Cruz, M.J.; Shi, D.; Gonen, T. Atomic resolution structure determination by the cryo-EM method MicroED. *Protein Sci.* **2017**, *26*, 8–15. [CrossRef]
11. Mitsuoka, K. Obtaining high-resolution images of biological macromolecules by using a cryo-electron microscope with a liquid-helium cooled stage. *Micron* **2011**, *42*, 100–106. [CrossRef] [PubMed]
12. Shelley, K.L.; Garman, E.F. Quantifying and comparing radiation damage in the Protein Data Bank. *Nat. Commun.* **2022**, *13*, 1314. [CrossRef] [PubMed]
13. Johansson, L.C.; Stauch, B.; Ishchenko, A.; Cherezov, V. A Bright Future for Serial Femtosecond Crystallography with XFELs. *Trends Biochem. Sci.* **2017**, *42*, 749–762. [CrossRef] [PubMed]
14. Chapman, H.N.; Fromme, P.; Barty, A.; White, T.A.; Kirian, R.A.; Aquila, A.; Hunter, M.S.; Schulz, J.; DePonte, D.P.; Weierstall, U.; et al. Femtosecond X-ray protein nanocrystallography. *Nature* **2011**, *470*, 73–77. [CrossRef] [PubMed]
15. Boutet, S.; Lomb, L.; Williams, G.J.; Barends, T.R.M.; Aquila, A.; Doak, R.B.; Weierstall, U.; DePonte, D.P.; Steinbrener, J.; Shoeman, R.L.; et al. High-Resolution Protein Structure Determination by Serial Femtosecond Crystallography. *Science* **2012**, *337*, 362–364. [CrossRef]
16. Weinert, T.; Olieric, N.; Cheng, R.; Brunle, S.; James, D.; Ozerov, D.; Gashi, D.; Vera, L.; Marsh, M.; Jaeger, K.; et al. Serial millisecond crystallography for routine room-temperature structure determination at synchrotrons. *Nat. Commun.* **2017**, *8*, 542. [CrossRef]
17. Nam, K.H. Room-Temperature Structure of Xylitol-Bound Glucose Isomerase by Serial Crystallography: Xylitol Binding in the M1 Site Induces Release of Metal Bound in the M2 Site. *Int. J. Mol. Sci.* **2021**, *22*, 3892. [CrossRef]

18. Tenboer, J.; Basu, S.; Zatsepin, N.; Pande, K.; Milathianaki, D.; Frank, M.; Hunter, M.; Boutet, S.; Williams, G.J.; Koglin, J.E.; et al. Time-resolved serial crystallography captures high-resolution intermediates of photoactive yellow protein. *Science* **2014**, *346*, 1242–1246. [CrossRef]
19. Orville, A.M. Recent results in time resolved serial femtosecond crystallography at XFELs. *Curr. Opin. Struct. Biol.* **2020**, *65*, 193–208. [CrossRef]
20. Pandey, S.; Calvey, G.; Katz, A.M.; Malla, T.N.; Koua, F.H.M.; Martin-Garcia, J.M.; Poudyal, I.; Yang, J.H.; Vakili, M.; Yefanov, O.; et al. Observation of substrate diffusion and ligand binding in enzyme crystals using high-repetition-rate mix-and-inject serial crystallography. *IUCrJ* **2021**, *8*, 878–895. [CrossRef]
21. Malla, T.N.; Schmidt, M. Transient state measurements on proteins by time-resolved crystallography. *Curr. Opin. Struct. Biol.* **2022**, *74*, 102376. [CrossRef] [PubMed]
22. Westenhoff, S.; Meszaros, P.; Schmidt, M. Protein motions visualized by femtosecond time-resolved crystallography: The case of photosensory vs photosynthetic proteins. *Curr. Opin. Struct. Biol.* **2022**, *77*, 102481. [CrossRef]
23. Worrall, J.A.R.; Hough, M.A. Serial femtosecond crystallography approaches to understanding catalysis in iron enzymes. *Curr. Opin. Struct. Biol.* **2022**, *77*, 102486. [CrossRef] [PubMed]
24. Schaffer, J.E.; Kukshal, V.; Miller, J.J.; Kitainda, V.; Jez, J.M. Beyond X-rays: An overview of emerging structural biology methods. *Emerg. Top. Life Sci.* **2021**, *5*, 221–230. [CrossRef] [PubMed]
25. Nam, K.H. Processing of Multicrystal Diffraction Patterns in Macromolecular Crystallography Using Serial Crystallography Programs. *Crystals* **2022**, *12*, 103. [CrossRef]
26. Nam, K.H. Sample delivery media for serial crystallography. *Int. J. Mol. Sci.* **2019**, *20*, 1094. [CrossRef] [PubMed]
27. Martiel, I.; Muller-Werkmeister, H.M.; Cohen, A.E. Strategies for sample delivery for femtosecond crystallography. *Acta Crystallogr. D Struct. Biol.* **2019**, *75*, 160–177. [CrossRef]
28. Grünbein, M.L.; Nass Kovacs, G. Sample delivery for serial crystallography at free-electron lasers and synchrotrons. *Acta Crystallogr. D Biol. Crystallogr.* **2019**, *75*, 178–191. [CrossRef]
29. Zhao, F.Z.; Zhang, B.; Yan, E.K.; Sun, B.; Wang, Z.J.; He, J.H.; Yin, D.C. A guide to sample delivery systems for serial crystallography. *FEBS J.* **2019**, *286*, 4402–4417. [CrossRef]
30. Kang, H.S.; Min, C.K.; Heo, H.; Kim, C.; Yang, H.; Kim, G.; Nam, I.; Baek, S.Y.; Choi, H.J.; Mun, G.; et al. Hard X-ray free-electron laser with femtosecond-scale timing jitter. *Nat. Photonics* **2017**, *11*, 708–713. [CrossRef]
31. Huang, N.; Deng, H.; Liu, B.; Wang, D.; Zhao, Z. Features and futures of X-ray free-electron lasers. *Innovation* **2021**, *2*, 100097. [CrossRef] [PubMed]
32. Eom, I.; Chun, S.H.; Lee, J.H.; Nam, D.; Ma, R.; Park, J.; Park, S.; Park, S.H.; Yang, H.; Nam, I.; et al. Recent Progress of the PAL-XFEL. *Appl. Sci.* **2022**, *12*, 1010. [CrossRef]
33. Park, J.; Kim, S.; Nam, K.H.; Kim, B.; Ko, I.S. Current status of the CXI beamline at the PAL-XFEL. *J. Korean Phys. Soc.* **2016**, *69*, 1089–1093. [CrossRef]
34. Kim, J.; Kim, H.Y.; Park, J.; Kim, S.; Kim, S.; Rah, S.; Lim, J.; Nam, K.H. Focusing X-ray free-electron laser pulses using Kirkpatrick-Baez mirrors at the NCI hutch of the PAL-XFEL. *J. Synchrotron Radiat.* **2018**, *25*, 289–292. [CrossRef]
35. Park, J.; Kim, S.; Kim, S.; Nam, K.H. Multifarious injection chamber for molecular structure study (MICOSS) system: Development and application for serial femtosecond crystallography at Pohang Accelerator Laboratory X-ray Free-Electron Laser. *J. Synchrotron Radiat.* **2018**, *25*, 323–328. [CrossRef] [PubMed]
36. Lee, D.; Baek, S.; Park, J.; Lee, K.; Kim, J.; Lee, S.J.; Chung, W.K.; Lee, J.L.; Cho, Y.; Nam, K.H. Nylon mesh-based sample holder for fixed-target serial femtosecond crystallography. *Sci. Rep.* **2019**, *9*, 6971. [CrossRef] [PubMed]
37. Park, J.; Park, S.; Kim, J.; Park, G.; Cho, Y.; Nam, K.H. Polyacrylamide injection matrix for serial femtosecond crystallography. *Sci. Rep.* **2019**, *9*, 2525. [CrossRef]
38. Lee, D.; Park, S.; Lee, K.; Kim, J.; Park, G.; Nam, K.H.; Baek, S.; Chung, W.K.; Lee, J.L.; Cho, Y.; et al. Application of a high-throughput microcrystal delivery system to serial femtosecond crystallography. *J. Appl. Crystallogr.* **2020**, *53*, 477–485. [CrossRef]
39. Lee, K.; Lee, D.; Baek, S.; Park, J.; Lee, S.J.; Park, S.; Chung, W.K.; Lee, J.L.; Cho, H.S.; Cho, Y.; et al. Viscous-medium-based crystal support in a sample holder for fixed-target serial femtosecond crystallography. *J. Appl. Crystallogr.* **2020**, *53*, 1051–1059. [CrossRef]
40. Lee, K.; Kim, J.; Baek, S.; Park, J.; Park, S.; Lee, J.-L.; Chung, W.K.; Cho, Y.; Nam, K.H. Combination of an inject-and-transfer system for serial femtosecond crystallography. *J. Appl. Crystallogr.* **2022**, *55*, 813–822. [CrossRef]
41. Lee, K.; Lee, D.; Park, J.; Lee, J.-L.; Chung, W.K.; Cho, Y.; Nam, K.H. Upgraded Combined Inject-and-Transfer System for Serial Femtosecond Crystallography. *Appl. Sci.* **2022**, *12*, 9125. [CrossRef]
42. DePonte, D.P.; Weierstall, U.; Schmidt, K.; Warner, J.; Starodub, D.; Spence, J.C.H.; Doak, R.B. Gas dynamic virtual nozzle for generation of microscopic droplet streams. *J. Phys. D* **2008**, *41*, 195505. [CrossRef]
43. Chrambach, A.; Rodbard, D. Polyacrylamide Gel Electrophoresis. *Science* **1971**, *172*, 440–451. [CrossRef] [PubMed]
44. Nam, K.H. Shortening injection matrix for serial crystallography. *Sci. Rep.* **2020**, *10*, 107. [CrossRef]
45. Nam, K.H. Polysaccharide-based injection matrix for serial crystallography. *Int. J. Mol. Sci.* **2020**, *21*, 3332. [CrossRef]
46. Nam, K.H. Lard injection matrix for serial crystallography. *Int. J. Mol. Sci.* **2020**, *21*, 5977. [CrossRef]
47. Nam, K.H. Beef tallow injection matrix for serial crystallography. *Sci. Rep.* **2022**, *12*, 694. [CrossRef]

48. Nam, K.H.; Park, S.; Park, J. Preliminary XFEL data from spontaneously grown endo-1,4-β-xylanase crystals from Hypocrea virens. *Acta Crystallogr. F Struct. Biol. Commun.* **2022**, *78*, 226–231. [CrossRef]
49. Oghbaey, S.; Sarracini, A.; Ginn, H.M.; Pare-Labrosse, O.; Kuo, A.; Marx, A.; Epp, S.W.; Sherrell, D.A.; Eger, B.T.; Zhong, Y.; et al. Fixed target combined with spectral mapping: Approaching 100% hit rates for serial crystallography. *Acta Crystallogr. D Struct. Biol.* **2016**, *72*, 944–955. [CrossRef]
50. Dasgupta, S.; Hammond, W.B.; Goddard, W.A. Crystal Structures and Properties of Nylon Polymers from Theory. *J. Am. Chem. Soc.* **1996**, *118*, 12291–12301. [CrossRef]
51. Teng, T.Y. Mounting of Crystals for Macromolecular Crystallography in a Freestanding Thin-Film. *J. Appl. Crystallogr.* **1990**, *23*, 387–391. [CrossRef]
52. Bhuvanesh, N.S.P.; Reibenspies, J.H. A novel approach to micro-sample X-ray powder diffraction using nylon loops. *J. Appl. Crystallogr.* **2003**, *36*, 1480–1481. [CrossRef]
53. Nam, K.H.; Cho, Y. Stable sample delivery in a viscous medium via a polyimide-based single-channel microfluidic chip for serial crystallography. *J. Appl. Crystallogr.* **2021**, *54*, 1081–1087. [CrossRef]
54. Nam, K.H.; Kim, J.; Cho, Y. Polyimide mesh-based sample holder with irregular crystal mounting holes for fixed-target serial crystallography. *Sci. Rep.* **2021**, *11*, 13115. [CrossRef]
55. Doak, R.B.; Nass Kovacs, G.; Gorel, A.; Foucar, L.; Barends, T.R.M.; Grunbein, M.L.; Hilpert, M.; Kloos, M.; Roome, C.M.; Shoeman, R.L.; et al. Crystallography on a chip—Without the chip: Sheet-on-sheet sandwich. *Acta Crystallogr. D Struct. Biol.* **2018**, *74*, 1000–1007. [CrossRef]
56. Huang, C.Y.; Olieric, V.; Ma, P.K.; Panepucci, E.; Diederichs, K.; Wang, M.T.; Caffrey, M. In meso in situ serial X-ray crystallography of soluble and membrane proteins. *Acta Crystallogr. D* **2015**, *71*, 1238–1256. [CrossRef]
57. Calvey, G.D.; Katz, A.M.; Zielinski, K.A.; Dzikovski, B.; Pollack, L. Characterizing Enzyme Reactions in Microcrystals for Effective Mix-and-Inject Experiments using X-ray Free-Electron Lasers. *Anal. Chem.* **2020**, *92*, 13864–13870. [CrossRef]
58. Vakili, M.; Bielecki, J.; Knoška, J.; Otte, F.; Han, H.J.; Kloos, M.; Schubert, R.; Delmas, E.; Mills, G.; de Wijn, R.; et al. 3D printed devices and infrastructure for liquid sample delivery at the European XFEL. *J. Synchrotron Radiat.* **2022**, *29*, 331–346. [CrossRef]
59. Knoška, J.; Adriano, L.; Awel, S.; Beyerlein, K.R.; Yefanov, O.; Oberthuer, D.; Pena Murillo, G.E.; Roth, N.; Sarrou, I.; Villanueva-Perez, P.; et al. Ultracompact 3D microfluidics for time-resolved structural biology. *Nat. Commun.* **2020**, *11*, 657. [CrossRef]